Chronic kidney disease leads to microglial potassium efflux and inflammasome activation in the brain

see commentary on page 1020

OPEN

Silke Zimmermann[1], Akash Mathew[1], Olga Bondareva[2], Ahmed Elwakiel[1], Klarina Waldmann[3], Shihai Jiang[1], Rajiv Rana[1], Kunal Singh[1], Shrey Kohli[1], Khurrum Shahzad[1], Ronald Biemann[1], Thomas Roskoden[4], Silke Diana Storsberg[5], Christian Mawrin[6], Ute Krügel[7], Ingo Bechmann[8], Jürgen Goldschmidt[9], Bilal N. Sheikh[2] and Berend Isermann[1]

[1]Institute of Laboratory Medicine, Clinical Chemistry and Molecular Diagnostics, University Hospital; Leipzig, Germany; [2]Helmholtz Institute for Metabolic, Obesity and Vascular Research (HI-MAG) of the Helmholtz Center Munich, Leipzig, Germany; [3]Institute of Clinical Chemistry and Pathobiochemistry, Medical Faculty, Otto-von-Guericke University Magdeburg, Magdeburg, Germany; [4]Institute of Anatomy, Medical Faculty, Otto-von-Guericke University Magdeburg, Magdeburg, Germany; [5]Institute of Anatomy, Brandenburg Medical School, Neuruppin, Germany; [6]Department of Neuropathology and Center for Behavioral Brain Sciences (CBBS), Otto-von-Guericke-University Magdeburg, Magdeburg, Germany; [7]Rudolf Boehm Institute of Pharmacology and Toxicology, Medical Faculty, Leipzig University, Leipzig, Germany; [8]Institute of Anatomy, Leipzig University, Leipzig, Germany; and [9]Leibniz Institute for Neurobiology, Magdeburg, Germany

Cognitive impairment is common in extracerebral diseases such as chronic kidney disease (CKD). Kidney transplantation reverses cognitive impairment, indicating that cognitive impairment driven by CKD is therapeutically amendable. However, we lack mechanistic insights allowing development of targeted therapies. Using a combination of mouse models (including mice with neuron-specific IL-1R1 deficiency), single cell analyses (single-nuclei RNA-sequencing and single-cell thallium autometallography), human samples and *in vitro* experiments we demonstrate that microglia activation impairs neuronal potassium homeostasis and cognition in CKD. CKD disrupts the barrier of brain endothelial cells *in vitro* and the blood-brain barrier *in vivo*, establishing that the uremic state modifies vascular permeability in the brain. Exposure to uremic conditions impairs calcium homeostasis in microglia, enhances microglial potassium efflux via the calcium-dependent channel $K_{Ca}3.1$, and induces p38-MAPK associated IL-1β maturation in microglia. Restoring potassium homeostasis in microglia using a $K_{Ca}3.1$-specific inhibitor (TRAM34) improves CKD-triggered cognitive impairment. Likewise, inhibition of the IL-1β receptor 1 (IL-1R1) using anakinra or genetically abolishing neuronal IL-1R1 expression in neurons prevent CKD-mediated reduced neuronal potassium turnover and CKD-induced impaired cognition. Accordingly, in CKD mice, impaired cognition can be ameliorated by either preventing microglia activation or inhibiting IL-1R-signaling in neurons. Thus, our data suggest that potassium efflux from microglia triggers their activation, which promotes microglia IL-1β release and IL-1R1–mediated neuronal dysfunction in CKD. Hence, our study provides new mechanistic insight into cognitive impairment in association with CKD and identifies possible new therapeutic approaches.

Kidney International (2024) **106,** 1101–1116; https://doi.org/10.1016/j.kint.2024.06.028

KEYWORDS: cognitive impairment; chronic kidney disease; cytokines; microglia-neuron crosstalk; potassium flux

Translational Statement

Chronic kidney disease (CKD) impairs cognition through poorly defined mechanisms. As kidney transplantation restores cognition, cognitive impairment in CKD is reversible. Here we identify a new pathway disrupting glia-neuron crosstalk in CKD. We use mouse models, single-cell analyses, human samples, and *in vitro* models to demonstrate that CKD triggers potassium efflux from microglia, resulting in microglia interleukin (IL)-1β release and IL-1β receptor 1 (IL-1R1)–mediated neuronal dysfunction. The potassium channel $K_{Ca}3.1$ inhibitor senicapoc (clinically tested in patients with Alzheimer disease) reduces microglia activation and improves cognition. Likewise, the IL-1R antagonist anakinra improves cognition. These studies identify a pathway impairing cognition in CKD, which is possibly therapeutically amendable.

While cognitive impairment is common in peripheral diseases such as chronic kidney disease (CKD), mechanistic insights and effective therapies are lacking.[1,2] The frequency of cognitive impairment and dementia is increased in patients at all stages of CKD.[3] Kidney transplantation reverses cognitive impairment, indicating that

Correspondence: *Berend Isermann or Silke Zimmermann, Institute of Laboratory Medicine, Clinical Chemistry and Molecular Diagnostics, University Hospital; Paul-List-Straße 13/15, 04103 Leipzig, Germany. E-mail: berend.isermann@medizin.uni-leipzig.de or silke.zimmermann@medizin.uni-leipzig.de*

Received 8 January 2024; revised 14 June 2024; accepted 24 June 2024; published online 30 July 2024

cognitive impairment driven by CKD is therapeutically amendable.[4–6] Yet mechanisms underlying microglia-neuron communication remain largely elusive. Microglia are in close proximity to neurons and modulate their function.[7] Thus, brain-derived neurotrophic factor conveys neuroprotective effects,[8,9] while cytokines, such as interleukin-1β (IL-1β), are generally thought to convey detrimental effects,[10–12] given for example the association of single nucleotide polymorphisms in the promotor of IL-1 and tumor necrosis factor-α (associated with increased expression of respective cytokines) with neurodegenerative diseases such as Alzheimer's disease and Parkinson's disease.[13] Yet, also neuroprotective effects of cytokines have been proposed.[13] These differences may stem from different cell models used, cell-specific effects of cytokines in the central nervous system, or different cytokine concentrations and kinetics.[14] Previous reports demonstrated a function of IL-1β receptor 1 (IL-1R1) in neuronal cells *ex vivo*[15] or impaired cognition in association with an exaggerated inflammatory response of microglia with increased IL-1β secretion.[16] Yet, the role of IL-1β and its receptor IL-1R1 for CKD-induced cognitive impairment remains unknown.

Inflammation in the brain on acute kidney injury is associated with a disruption of the blood-brain barrier (BBB).[17,18] We speculated that chronic low-grade inflammation, as present in CKD, may likewise disrupt BBB function, allow uremic toxins to reach brain cells, and consecutively impair cognitive functions.[19–21] Considering the abundance of accumulated toxins in CKD, targeting individual toxins is not a feasible approach.[22] One commonality of peripheral diseases associated with cognitive impairment (e.g., liver or kidney failure) is sterile inflammation.[23–25] A known inducer of sterile inflammation is potassium efflux.[26] Hence, we speculated that modulation of potassium efflux from microglia may be an important step in microglia activation and CKD-induced cognitive impairment. However, whether potassium turnover in microglia is altered in CKD, which potassium channels are involved, and whether restoring microglia function protects from impaired cognition in CKD remain unknown.

METHODS

Additional details for methods are provided in the Supplementary Methods.

Mice

Wild-type mice (C57BL/6, 8 weeks old) were obtained from Janvier Labs. NLRP3$^{-/-}$ mice have been described before.[27,28] Mice had been backcrossed onto the C57BL/6 background for at least 9 generations. All animal experiments were conducted according to standards and procedures approved by the local Animal Care and Use Committee (Landesverwaltungsamt Halle and Landesverwaltungsamt Leipzig). Animal care and treatment were conducted in conformity with institutional guidelines that are in compliance with international laws and politics. The permission of the animal protection commission was given.

We generated new mouse models. In detail, we obtained embryonic stem cells from Eucomm containing mutant IL-1R1 with the potential to generate conditional knockout mice using the Cre-LoxP approach. These embryonic stem cells were successfully injected into oocytes, giving rise to several founder mouse lines. Founder mice were identified using complimentary polymerase chain reaction (PCR) strategies analysing the 5′-, 3′-, and middle region of the targeted gene locus (representative PCRs shown in Supplementary Figure S4, tail DNA was used for genotyping by PCR; for primers, see Supplementary Table S3). Confirmed founder mice were crossed with ubiquitously expressing flippase mice—ubiquitously expressing an enhanced variant of *Saccharomyces cerevisiae* FLiPase recombinase under the control of the human β-actin promoter (transgenic B6.Cg-Tg [ACTFlpE]9205Dym/J mice obtained from Jackson Laboratories)—to delete the LacZ-stop sequence. After genetic deletion of the LacZ-stop sequence (which conveys a complete knockout), we obtained conditional knockout mice for IL-1R (IL-1R^{LoxP}), which were again identified by PCR. These mice were crossed with Emx^{Cre} (neuronal Cre-expression) mice.

CKD mouse model (5/6 nephrectomy model)

5/6 nephrectomy was induced in a 2-step surgical procedure: (i) ablation of 2 of 3 of the kidney parenchyma of the right kidney in 6- to 8-week-old mice, (ii) followed 7 days later by complete nephrectomy of the contralateral kidney.[29]

Cell culture

Immortalized murine microglia cells (SIM-A9, ATCC CRL-3265) and murine neuronal cells (Neuro-2, Cell Lines Service, 400394) were maintained at 37 °C in cell culture media (microglia: DMEM/F-12, Fisher Scientific, 10% heat inactivated fetal bovine serum, 5% heat inactivated horse serum; neurons: EMEM, ATCC, 10% fetal bovine serum). For experiments, Neuro-2a cells were differentiated to neuronal cells by serum-starvation (2% fetal bovine serum) for 5 days prior to the experiment.[30] Cell lines routinely tested negative for mycoplasma. Cells were cultured in 10-cm^2 dishes and treated as follows: microglia were incubated for 6 hours with stimuli (10% control plasma or 10% CKD plasma, and in some experiments, cells were pre-stimulated for 1 hour with triarylmethane-34 (TRAM34; 100 nmol/L) or anakinra (10 mmol/L), followed by removal of medium, adding of fresh medium and further incubation for 12 hours to generate conditioned medium (CM). The CM was harvested, centrifuged at 300*g* for 5 minutes, and the supernatant added to the neuronal cells for a period of 24 hours. For detection of calcium dyshomeostasis, microglia were preloaded with Cal-520 (Abcam; 5 μmol/L) prior to incubation with control or CKD plasma.

Statistical analysis

Mice were grouped according to genotype and randomly assigned to different interventions (sham, nephrectomy,

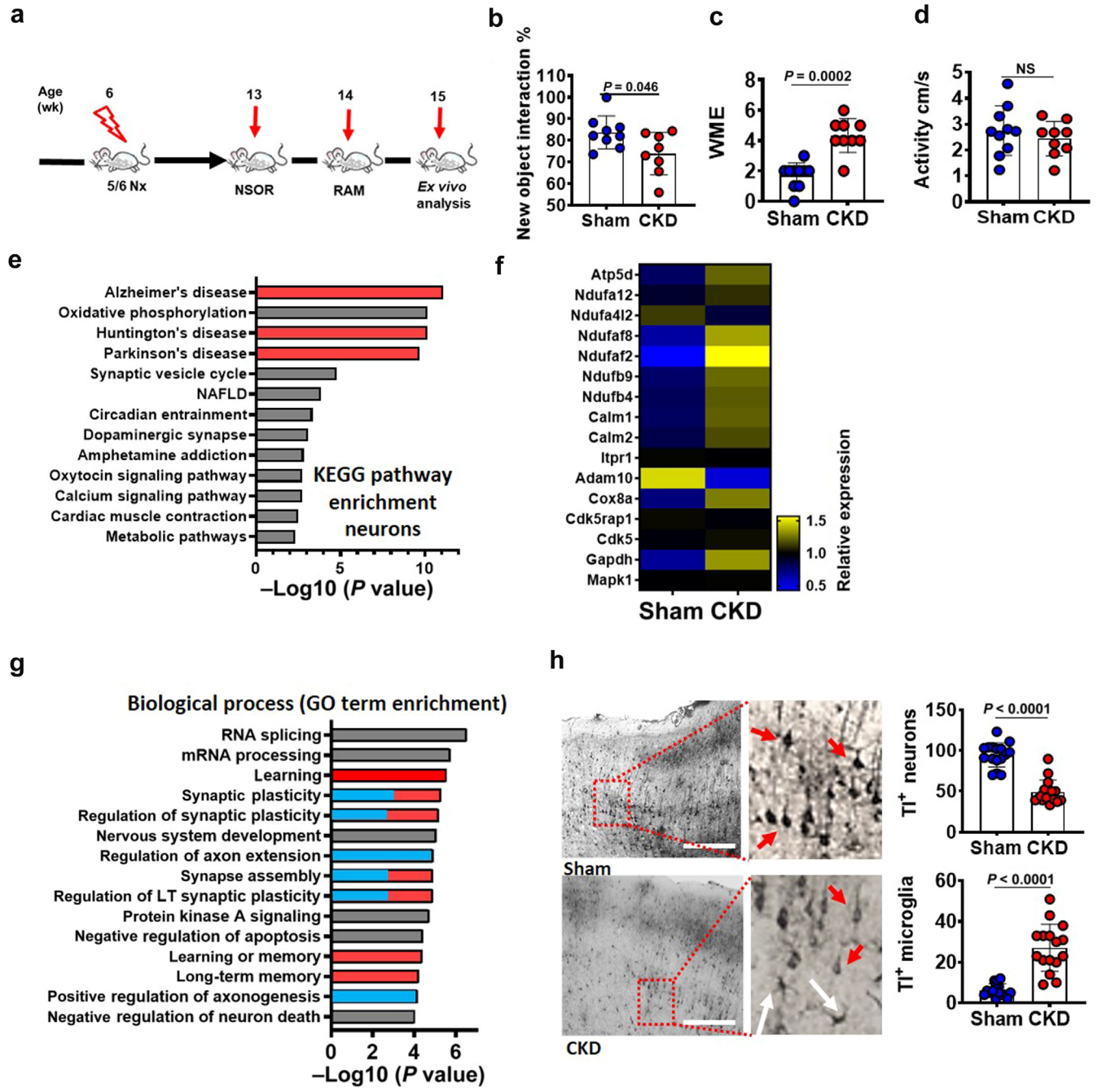

Figure 1 | Chronic kidney disease (CKD) impairs cognition in association with increased microglial potassium efflux. (**a**) Scheme of experimental approach (5/6 nephrectomy [5/6 Nx]) to induce CKD in mice. (**b**–**d**) Cognition, as determined by nonspatial object recognition (NSOR; the results are reported as the percentage of time spent with the new unknown object) (**b**) and radial arm maze (RAM; the results are reported as working memory errors [WMEs]) (**c**) tests in wild-type sham-operated control (sham) and CKD mice. (**d**) Bar graph showing activity of the mice (in cm/s) in the NSOR. (**e,f**) Pathway analyses (Kyoto Encyclopedia of Genes and Genomes [KEGG] analysis, $\log_{10}$ of P values [$P < 0.05$] obtained after correcting for multiple testing by Benjamini-Hochberg) (**e**) and heatmap (**f**) of Alzheimer's disease–associated differentially expressed genes (DEGs) in neurons of brains of CKD versus sham mice (single-nuclei RNA-sequencing analyses, n = 3 per condition). (**g**) Top enriched terms obtained from Gene Ontology (GO) terms of biological process pathway analyses based on DEGs within the neuronal cluster of CKD mice compared to sham-operated mice (n = 3). The $\log_{10}$ of P values ($P < 0.05$) obtained after correcting for multiple testing (Benjamini-Hochberg correction) are shown. Red bars: biological process associated with learning and synaptic formation or neuron and axon biology. (**h**) Example images (left) and bar graph (mean ± SEM, each dot represents number of positive cells in 1 field of view; data from 4 different mice per group) with dot plot (right) summarizing thallium-positive (Tl^+) cells in *ex vivo* thallium autometallography. (**b–d,h**) P values were determined using 2-tailed Student's t test. (**h**) bar = 500 µm. Arrows depict microglia (white) or neurons (red). LT, long-term; NAFLD, nonalcoholic fatty liver disease; NS, not significant. To optimize viewing of this image, please see the online version of this article at www.kidney-international.org.

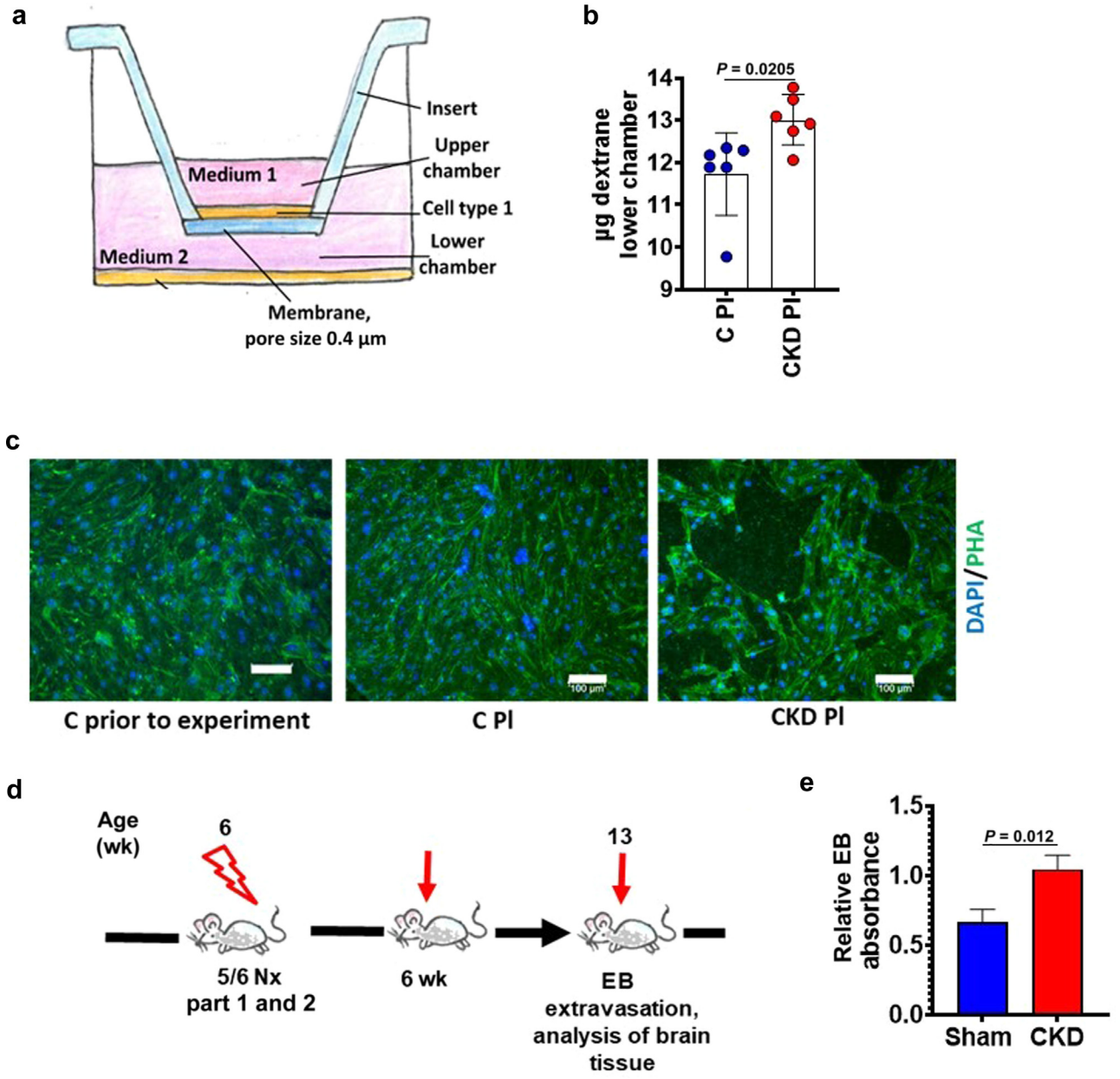

Figure 2 | Blood-brain barrier disruption in chronic kidney disease (CKD). (**a**) Scheme of the *in vitro* blood-brain barrier model: Boyden chamber with brain endothelial cells (b.End3, cell-type 1) seeded on the insert surface. Dextran (4.4 kDa tetramethyl rhodamine isothiocyanate–conjugated) was added to the upper chamber. (**b**) Bar graph (mean ± SEM) summarizing the amount of dextran in the lower chamber of the Boyden chamber. *P* values determined using 2-tailed Student's *t* test. (**c**) Representative immunofluorescence images of murine brain endothelial cells (b.End3) stained for phalloidin (PHA, green) prior to the experiment or following exposure to plasma from healthy controls (C PI) or plasma from patients with CKD (CKD PI); 4′,6-diamidino-2-phenylindole (DAPI) was used as the nuclear counterstain. Bar = 100 µm. (**d**) Experimental scheme and timeline of Evans blue (EB) extravasation test. (**e**) Bar graph (mean ± SEM) summarizing the relative absorbance of EB in brain tissue of sham or CKD mice. *P* values determined 2-tailed Student's *t* test. 5/6 Nx, 5/6 nephrectomy. To optimize viewing of this image, please see the online version of this article at www.kidney-international.org.

TRAM34). Data are summarized as the mean ± SEM. Statistical analyses were performed with Student's *t* test or 1-way analysis of variance (ANOVA), as appropriate, and indicated in the figure legends. *Post hoc* comparisons of ANOVA were corrected with the method of Dunnett multiple comparison. The Kolmogorov–Smirnov test or D'Agostino–Pearson normality test was used to determine whether the data were consistent with a Gaussian distribution. Prism 8 (GraphPad Software; www.graphpad.com) software was used for statistical analyses. Values of $P \leq 0.05$ were considered statistically significant. Statistical analyses are mentioned in the Data Supplement for analyses of RNA-sequencing (RNA-seq) data and in the corresponding figure legends.

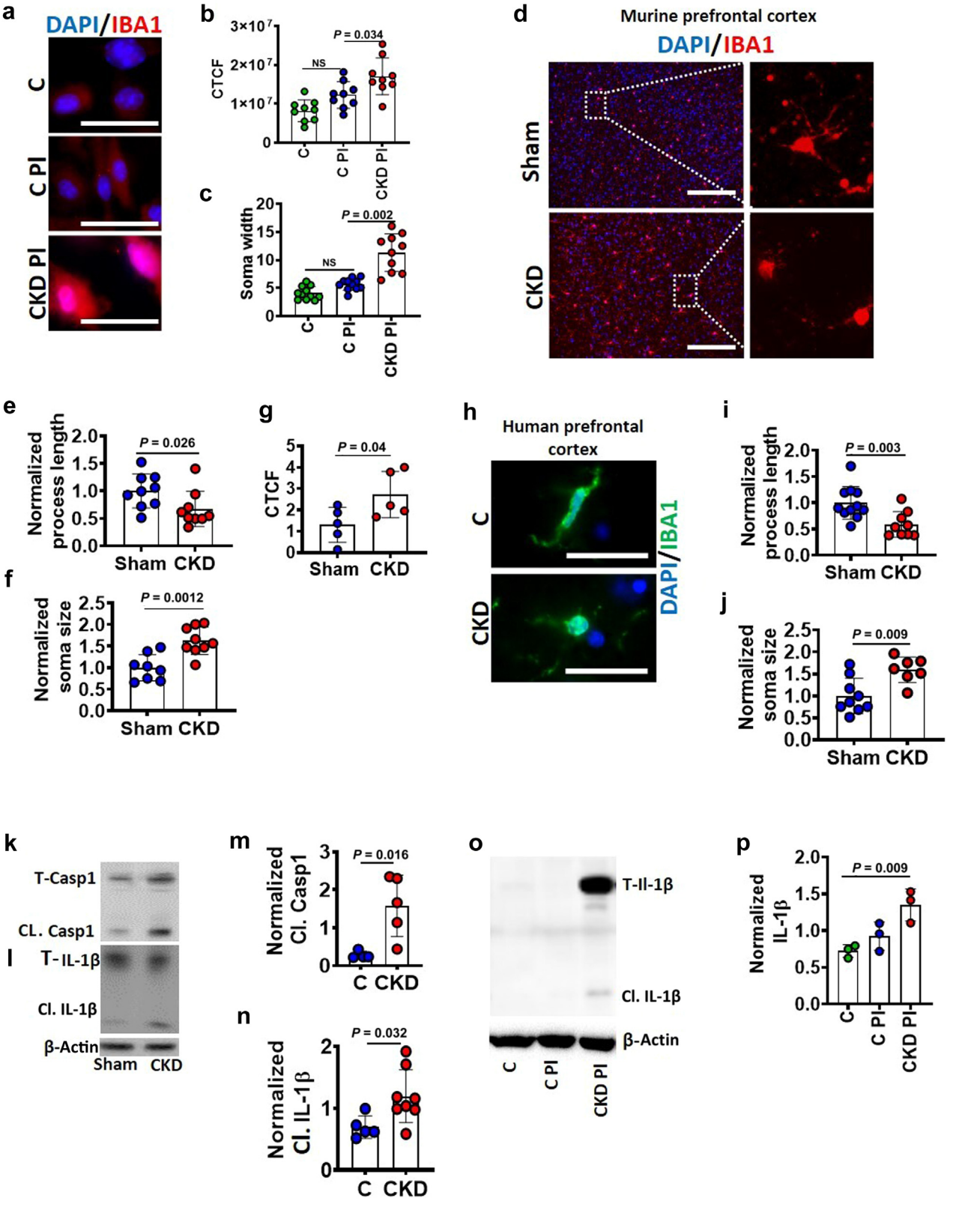

Figure 3 | Microglia activation in chronic kidney disease (CKD). (**a–c**) Representative images of murine microglia exposed to control plasma (C PI) or CKD plasma (CKD PI) and stained for ionized calcium-binding adapter molecule 1 (Iba1; 4′,6-diamidino-2-phenylindole [DAPI] nuclear counterstain, blue) (**a**) and bar graphs with dot plot summarizing the corrected total cell IBA1 fluorescence (CTCF) (**b**) and soma width (**c**). Bar = 50 μm; dots summarize mean ± SEM; each dot represents the analysis of 1 field of view of in total 3 biological replicates. *P* values determined by 1-way analysis of variance with Dunnett *post hoc* comparison. (**d–g**) Representative images of Iba1 immunohistochemistry in the brains of control and CKD mice (**d**) (bar = 50 μm) and (**d–g**) bar graphs (mean ± SEM, each dot represents analysis of 1 field of view of in total 3 independent experiments) representing normalized process length (**e**) and soma width (**f**) and CTCF (continued)

RESULTS

CKD impairs cognition in association with potassium efflux in microglia and neurons

To gain insights into the cell-specific molecular pathways in CKD-triggered cognitive impairment, we subjected C57Bl/6 mice to 5/6 nephrectomy. The 5/6 nephrectomy model mimics CKD (mice referred to as CKD mice; Figure 1a; Supplementary Figure S1A).[31,32] Kidney retention parameters (urea and creatinine) were increased in CKD mice, confirming impaired kidney function (Supplementary Figure S1B and C). To avoid an impact of increased blood pressure, the impact of CKD on cognition and the brain was determined within 8 weeks post 5/6 nephrectomy, because mice have been reported to maintain normal blood pressure during this period.[29] To screen for possible behavior changes in CKD mice we used the nonspatial object recognition test (NSOR) and the radial arm maze (RAM), established assays for impaired learning and memory (Figure 1a).[33,34] In both assays, CKD mice performed worse than age- and sex-matched control mice, as reflected by a lesser interaction with a novel object and more working memory errors in the NSOR and RAM, respectively (Figure 1b and c). Spontaneous activity was comparable in control and CKD mice, indicating that the impaired cognitive performance does not result from reduced mobility in CKD mice (Figure 1d).

To determine cell-specific alterations associated with impaired cognition in CKD mice, we conducted single-nuclei RNA-sequencing (snRNA-seq) analysis of cortices (Supplementary Figures S1D–F and S2; Supplementary Table S1). KEGG (Kyoto Encyclopedia of Genes and Genomes) pathway analyses revealed that among the 4 most induced pathways in neuronal cell clusters from CKD mice 3 were related to Alzheimer's disease, Huntington's disease, and Parkinson's disease, congruent with neurodegenerative processes in CKD mice (Figure 1e and f). GO (Gene Ontology) term enrichment identified among the 15 most-regulated biological processes 7 that were associated with learning and synaptic formation in CKD mice or were related to neuron and axon biology (Figure 1g, red [biological process associated with learning and synaptic formation or neuron and axon biology]), corroborating the idea that CKD impairs neuronal function (Figure 1g).

To determine whether neuronal function is altered in CKD mice, we applied thallium autometallography (TlAMG), which enables visualization of potassium turnover and hence reflects neuronal function at the single-cell level (Supplementary Figure S3).[35] TIAMG staining of neurons was reduced in CKD mice compared to controls (Figure 1h), reflecting reduced neuronal potassium turnover and impaired neuronal function. Intriguingly, reduced neuronal TlAMG staining was associated with a marked increased TlAMG staining in microglia. The increased TlAMG staining in microglia implies increased microglial potassium efflux, which may reflect microglia activation (Figure 1h).

BBB disruption in CKD

The altered gene expression and neuronal and microglia activation (as indicated by TIAMG) raises the question as to whether the BBB is impaired in CKD. To determine the impact of CKD on BBB integrity, we first used an *in vitro* BBB model. Brain endothelial cells (b.End3) were seeded onto a Boyden chamber (Figure 2a) until they formed a tight monolayer (after 4 days). Cells were then exposed to plasma from healthy controls or patients with CKD and dextran (4.4 kDa tetramethyl rhodamine isothiocyanate–conjugated) permeability was determined. Uremic plasma increased the dextran permeation into the lower chamber (Figure 2b). Loss of a tight monolayer was also visible on immunofluorescence staining (Figure 2c).

To validate our findings *in vivo*, we used the 5/6 nephrectomy model (CKD mice) and assessed Evans blue extravasation into the brain to determine BBB leakage (Figure 2d).[36] Evans blue extravasation into the brain parenchyma, reflecting impaired BBB-function, was increased in CKD mice as compared to sham control mice in the absence of additional stimuli (Figure 2e). The impaired BBB function in CKD mice indicates that uremic toxins may cross the BBB and affect the function of brain cells.

Microglia activation in CKD

To scrutinize microglial activation in uremic conditions *in vitro*, we exposed microglia to the plasma of human patients with CKD or controls with normal kidney function (Supplementary Table S2). CKD plasma induced ionized calcium-binding adapter molecule 1 (Iba1) expression (Figure 3a and b; Supplementary Figure S4A) and enlarged microglial somata (Figure 3c), both indicating microglia activation. Likewise, Iba1 immunohistochemistry revealed shorter processes, larger somata of microglia and increased Iba1 fluorescence in CKD mice (Figure 3d–g; Supplementary Figure S4B), indicating microglia activation.[37,38] snRNA-seq analysis showed upregulation of *Iba1*, *C1qa*, and *Ctss* in microglia, corroborating microglia activation in CKD (Supplementary Figure S4C). Not surprisingly, the snRNA-seq analyses suggest possible involvement of other cells in addition to microglia. For example, based on snRNA-seq

Figure 3 | (continued) of Iba1 fluorescence (**g**) of murine microglia. Two-tailed Student's *t* test was used. (**h–j**) Representative images of IBA1-immunofluorescence in brains of controls and patients with CKD (**h**) and bar graphs summarizing results of microglia process length (**i**) and soma size (**j**). Each dot represents 1 field of view of in 4 patients. (**k–n**) Representative immunoblots of caspase-1 (Casp1) (**k**) and interleukin-1β (IL-1β) (**l**) in brain lysates (prefrontal cortex) from sham and CKD mice. Total (T) and cleaved (Cl.) forms are shown. Bar graphs (mean ± SEM, each dot represents 1 brain) summarizing immunoblot results of cleaved caspase 1 (Cl. Casp1) (**m**) and IL-1β (Cl. IL-1β) (**n**) in brain lysates of sham and CKD mice. Two-tailed Student's *t* test was used. (**o,p**) Representative immunoblot of IL-1β (**o**) and bar graph summarizing results (each dot represents 1 biological sample) (**p**) in SIM-A9 cells treated with control medium (C), C Pl, or CKD Pl. *P* values were determined using Mann-Whitney test. NS, not significant. To optimize viewing of this image, please see the online version of this article at www.kidney-international.org.

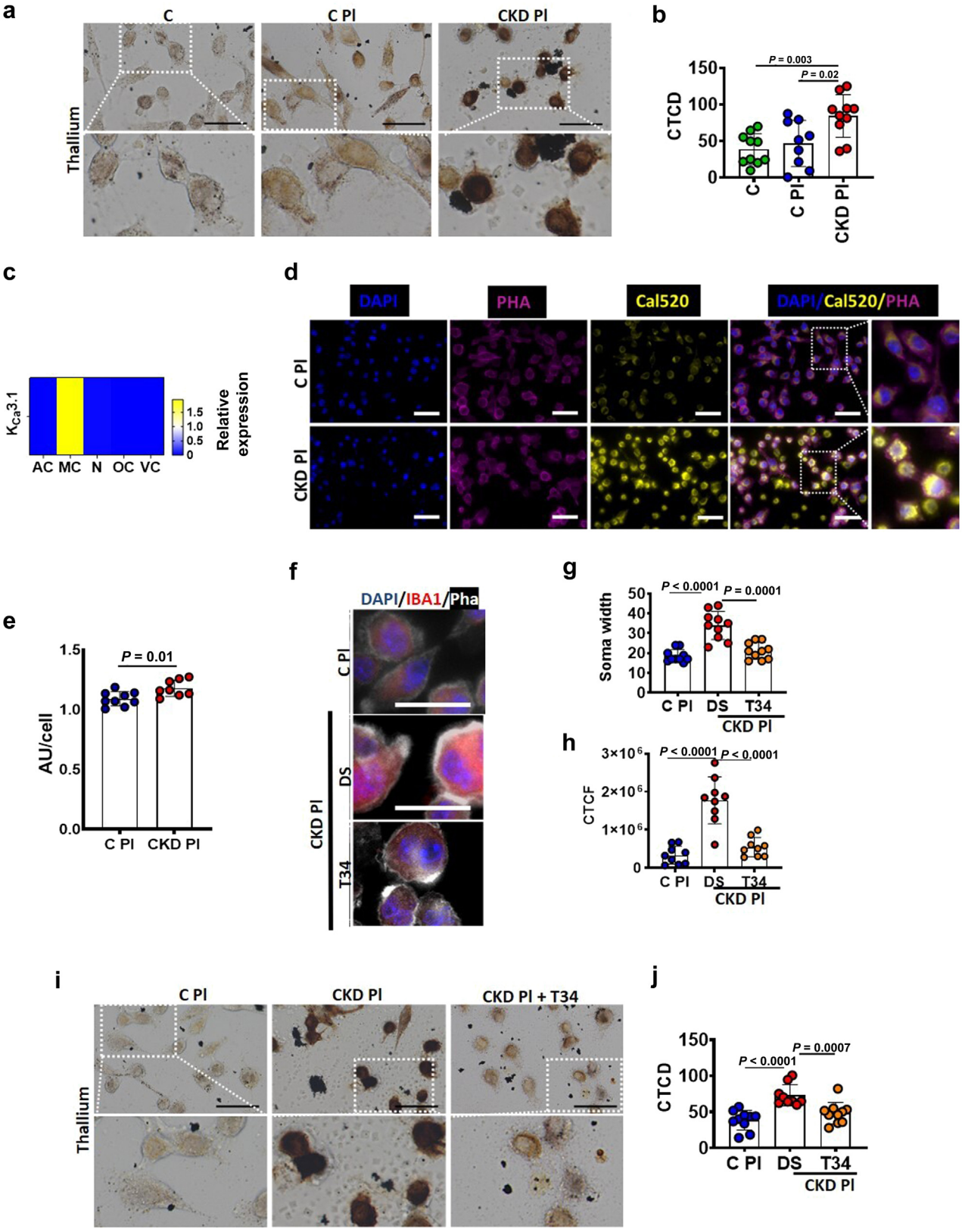

Figure 4 | Priming of microglia in chronic kidney disease (CKD) depends on potassium efflux. (**a,b**) Representative images (**a**) and bar graph with dot plot summarizing the corrected total cell density (CTCD) (**b**) of thallium autometallographically stained murine microglia (SIM-A9) exposed to control plasma or CKD plasma with or without pretreatment with triarylmethane-34 ([TRAM34, T34]; control: vehicle dimethylsulfoxide [DMSO, DS]). Bar = 50 μm; *P* values were determined using 1-way analysis of variance (ANOVA) with Dunnett *post hoc* comparison. (**c**) $K_{Ca}3.1$ expression levels in in single-nuclei RNA-sequencing data of murine brain (n = 3). (**d,e**) Exemplary immunofluorescence images of (continued)

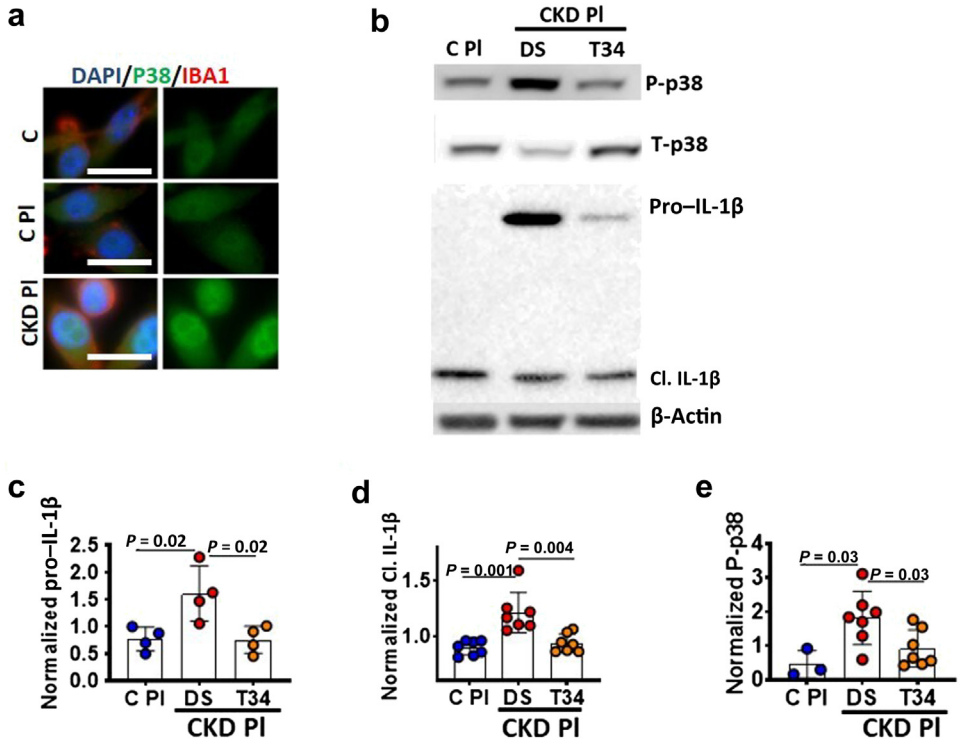

Figure 5 | Triarylmethane-34 (TRAM34, T34) leads to reduced interleukin-1β (IL-1β) cleavage in microglia. (**a**) Example of cytoimmunofluorescence images. Microglia were exposed to normal medium (control [C]) or to plasma obtained from controls (C PI) or patients with CKD (CKD PI) and stained for p38 (green) and ionized calcium-binding adapter molecule 1 ([IBA1], red; 4′,6-diamidino-2-phenylindole [DAPI], nuclear counterstain, blue). Bars = 50 μm. (**b**) Representative Western blot of phospho-p38 (P-p38), total p38 (T-p38), pro–Il-1β, and cleaved Il-1β ([Cl. Il-1β], loading control: β-actin) in microglial exposed to C PI or CKD PI with T34 or without T34 (solvent only, dimethylsulfoxide [DMSO, DS]). (**c–e**) Bar graphs (mean ± SEM, each dot represents 1 biological replicate) summarizing levels of pro–Il-1β, Cl. IL-1β, and P-p38 in microglia exposed to control or uremic plasma without or with T34 treatment. *P* values were determined using 1-way ANOVA with Dunnett *post hoc* comparison. To optimize viewing of this image, please see the online version of this article at www.kidney-international.org.

data, astrocytes increased in number (Supplementary Figure S4D). Increased expression of the hemoglobin scavenger CD163 by various brain cells is a marker of severe impaired blood brain integrity (e.g., in diseases associated with intracranial hemorrhage).[39] On CD163 immunohistochemistry, we observed punctured staining of CD163 in the brain (Supplementary Figure S4E), which contrasts with published data, showing a more even staining of cells.[40]

In endothelial cells, KEGG pathway analyses revealed that top pathways differentially regulated are related to basic cellular functions, such as oxidative phosphorylation, RNA-processing or proteostasis (Supplementary Figure S5A and B), which is congruent with endothelial dysfunction and an impairment of the BBB. Of note, in endothelial cells and microglia, pathways related to neurodegeneration were highly represented (Supplementary Figure S5A and B, 6 of the top 20 pathways in each cell type), supporting the notion that CKD impairs the BBB and triggers an interaction of activated microglia and neurons, which promotes a neurodegenerative process. Given the close interaction of microglia and neurons,[41,42] we focused on the interaction of these cells.

To scrutinize microglial activation *in vivo*, we used intravital microscopy in transgenic mice expressing enhanced green fluorescent protein under the CXC3R1 (C-X3-C motif

Figure 4 | (continued) microglia stained with (**d**) Cal-520 (yellow), 4′,6-diamidino-2-phenylindole (DAPI, nuclear counterstain, blue), and phalloidin (PHA, purple), and bar graphs with dot plot (mean ± SEM, each dot represents the analysis of 1 field of view of 3 independent experiments) summarizing microglia calcium content (represented as AU) (**e**). Microglia were cultured with control plasma (C PI) or CKD plasma (CKD PI) following preloading with Cal-520 for 45 minutes. Bar = 50 μm. *P* values were determined using 2-tailed Student's *t* test. (**f–h**) Exemplary immunofluorescence images of microglia stained with (**f**) ionized calcium-binding adapter molecule 1 (IBA1, red), DAPI (nuclear counterstain, blue), and PHA (white), and bar graphs with dot plot (mean ± SEM, each dot represents the analysis of 1 field of view of 3 independent experiments) summarizing microglia cell soma width (**g**) and IBA1 staining intensity (represented as corrected total cell fluorescence [CTCF]) (**h**). Microglia were cultured with C PI or CKD PI without (vehicle control, DS) or with T34 pretreatment. Bar = 50 μm. *P* values were determined using 1-way ANOVA with Dunnett *post hoc* comparison. (**i,j**) Example images (**i**) and bar graph with dot plot summarizing the CTCD (**j**) of thallium-autometallographically stained murine microglial (SIM-A9) exposed to C PI or CKD PI with or without pretreatment with T34 (control: vehicle DS). Bar = 50 μm. *P* values were determined using 1-way ANOVA with Dunnett *post hoc* comparison. AC, astrocytes; MC, microglia cell; N, neurons; OC, oligodendrocytes; VC, vascular cells. To optimize viewing of this image, please see the online version of this article at www.kidney-international.org.

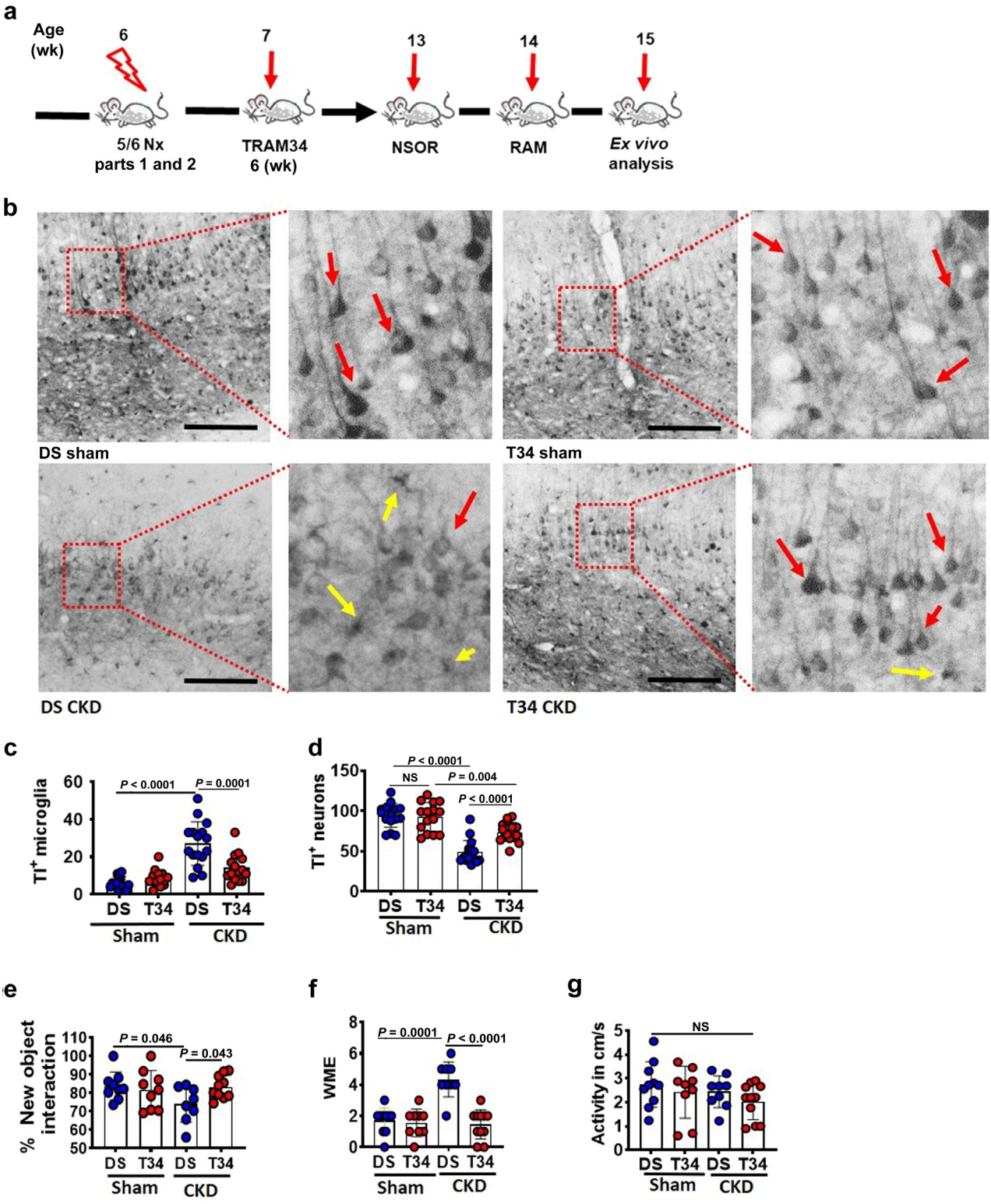

Figure 6| Triarylmethane-34 (TRAM34, T34) ameliorates microglial potassium efflux and behavior in chronic kidney disease (CKD). (**a**) Scheme summarizing experimental *in vivo* approach. Post CKD induction, a subgroup of mice received TRAM34 for further 6 weeks, followed by nonspatial object recognition (NSOR) and radial arm maze (RAM) test and tissue harvest. (**b–d**) Example images (**b**) and bar graph (mean ± SEM, each dot represents number of positive cells in 1 field of view; data from 4 different mice per group) with dot plot (**c,d**) summarizing thallium-positive (Tl^+) cells in *ex vivo* thallium autometallography from sham-operated control and CKD mice treated with vehicle dimethylsulfoxide (DMSO, DS) or T34. Each dot represents the count of the respective cell type in 1 field of view. *P* values were determined using 1-way analysis of variance (ANOVA) with Dunnett *post hoc* comparison; bar = 500 μm (**b**). Arrows depict microglia (yellow) or neurons (red). (**e–g**) Cognition, as determined by NSOR (the results are reported as the percentage of time spent with the new unknown (continued)

chemokine receptor 1) promoter, allowing *in vivo* imaging of microglia. Using this model we observed more microglial phagocytic cups, larger somata, and increased process motility (Supplementary Figure S6A–D) in brains of CKD mice, reflecting increased activation of microglia.[43] Likewise, we detected microglia activation in patients with CKD using IBA1 immunohistochemistry, which showed an increase of morphologically activated microglia in brain sections of patients with CKD compared to individuals without CKD (Figure 3h–j; Supplementary Table S3). Taken together, these results demonstrate that CKD is associated with microglia activation.

Microglia control sterile inflammation, including that related to NOD-, LRR- and pyrin domain-containing protein 3 (NLRP3) inflammasome activation.[44,45] Indeed, activated (cleaved) caspase-1 and IL-1β levels were increased in the cortices of CKD versus control mice (Figure 3k–n). To determine whether CKD-related mediators induce IL-1β release from microglia, we treated microglia (murine SIM-A9 cell line) *in vitro* with control or CKD plasma for 6 hours, followed by media change and incubation for 12 hours with normal media. IL-1β levels in the supernatant obtained from the last 12 hours were increased in cells exposed to CKD plasma as compared to plasma of healthy controls (Figure 3o and p). These results indicate activation of microglia, as determined by IL-1β secretion in CKD conditions, which may contribute to cognitive impairment.

Priming of microglia in CKD depends on potassium efflux and its restoration improves cognition in CKD

An important step of inflammasome activation in professional inflammatory cells, including microglia, is the priming of gene expression of relevant genes. This priming step has been linked to potassium efflux. As (i) potassium dyshomeostasis in microglia is linked to p38 activation,[46] (ii) as activation of the p38 pathways increases IL-1β mRNA and pro–IL-1β in monocytes,[47] and (iii) as TlAMG revealed microglial potassium efflux (Figure 1h), we hypothesized that microglial potassium efflux from microglia is required for p38-mediated priming and subsequent IL-1β activation. *In vitro*, CKD plasma induced a strong accumulation of Tl^+ in microglial as compared to cells exposed to control plasma, indicating an increased potassium efflux (Figure 4a and b), analogously to the *ex vivo* results (Figure 1h). This raises the question as to whether the CKD plasma-induced potassium efflux triggers IL-1β expression, possibly via mitogen-activated protein kinase signaling.

To corroborate a role of potassium efflux for mitogen-activated protein kinase signaling and IL-1β induction in microglia we targeted the calcium-dependent potassium channel $K_{Ca}3.1$, which has been linked with microglia activation.[48–50] Corroborating the data of Kaushal et al,[50] the calcium-dependent potassium channel $K_{Ca}3.1$ is predominantly expressed in microglia but is not or only at low levels expressed in other brain cells (Figure 4c). Because the $K_{Ca}3.1$ channel is a Ca^{2+}-dependent potassium gate, its activation requires an increase of intracellular Ca^{2+} concentration. CKD plasma increases intracellular Ca^{2+} levels in microglia (Figure 4d and e), which is consistent with activation of the calcium-dependent $K_{Ca}3.1$ channel in CKD conditions.

To inhibit $K_{Ca}3.1$, we used TRAM34, which crosses the BBB,[50–52] and thus enabled us to evaluate a possible role of potassium efflux in CKD-induced microglia activation (Figure 4f–j). First, we confirmed that TRAM34 prevents CKD plasma-induced potassium efflux in microglia (Figure 4f–j; Supplementary Figure S7). Uremic (CKD) plasma induced p38 immunofluorescence (Figure 5a), but the inhibition of potassium efflux by TRAM34 reduced p38 phosphorylation, pro–IL-1β expression, and cleaved IL-1β levels in microglia stimulated with CKD plasma *in vitro* (Figure 5b–e). These data indicate that CKD induces potassium efflux from microglia, activating mitogen-activated protein kinase signaling and priming IL-1β induction.

TRAM34 ameliorates potassium efflux and behavior in CKD

Given the efficacy of TRAM34 in preventing microglia activation *in vitro* and its *in vivo* efficacy,[53,54] we next addressed whether preventing microglia potassium efflux by TRAM34 prevents microglia activation *in vivo* and preserves cognition in CKD mice. To this end, we treated 7-week-old CKD (5/6 nephrectomized) wild-type mice for a 6-week post CKD induction with TRAM34 (Figure 6a). TRAM34 reduced microglial thallium uptake (Figure 6b and c), indicating that it prevented CKD-induced potassium efflux. Remarkably, this was associated with improved neuronal thallium uptake (Figure 6b and d) and memory function in CKD mice (Figure 6e and f), suggesting that preventing microglia potassium efflux prevents impaired cognition in CKD mice. The activity between treated and untreated mice was comparable (Figure 6g).

Uremia-induced reduced neuronal potassium turnover depends on microglia-neuron crosstalk via IL-1R1

The above observations support a model in which $K_{Ca}3.1$ promotes potassium efflux from microglial, priming microglial for IL-1β maturation and release, thus impairing neuronal function and cognition in CKD. To further validate this model, we exposed neurons to plasma from healthy controls of patients with CKD and determined Tl^+ uptake as a measure of neuronal activation. Neither plasma altered Tl^+

Figure 6 | (continued) object) (**e**) and RAM (the results are reported as working memory errors [WMEs]) (**f**) tests in sham-operated control (sham) and CKD mice treated with vehicle (DS) or T34, while the overall activity in the NSOR test was comparable (**g**). The results are represented as bar graphs, with each dot representing 1 mouse. *P* values were determined using 1-way ANOVA with Dunnett *post hoc* comparison. NS, not significant. To optimize viewing of this image, please see the online version of this article at www.kidney-international.org.

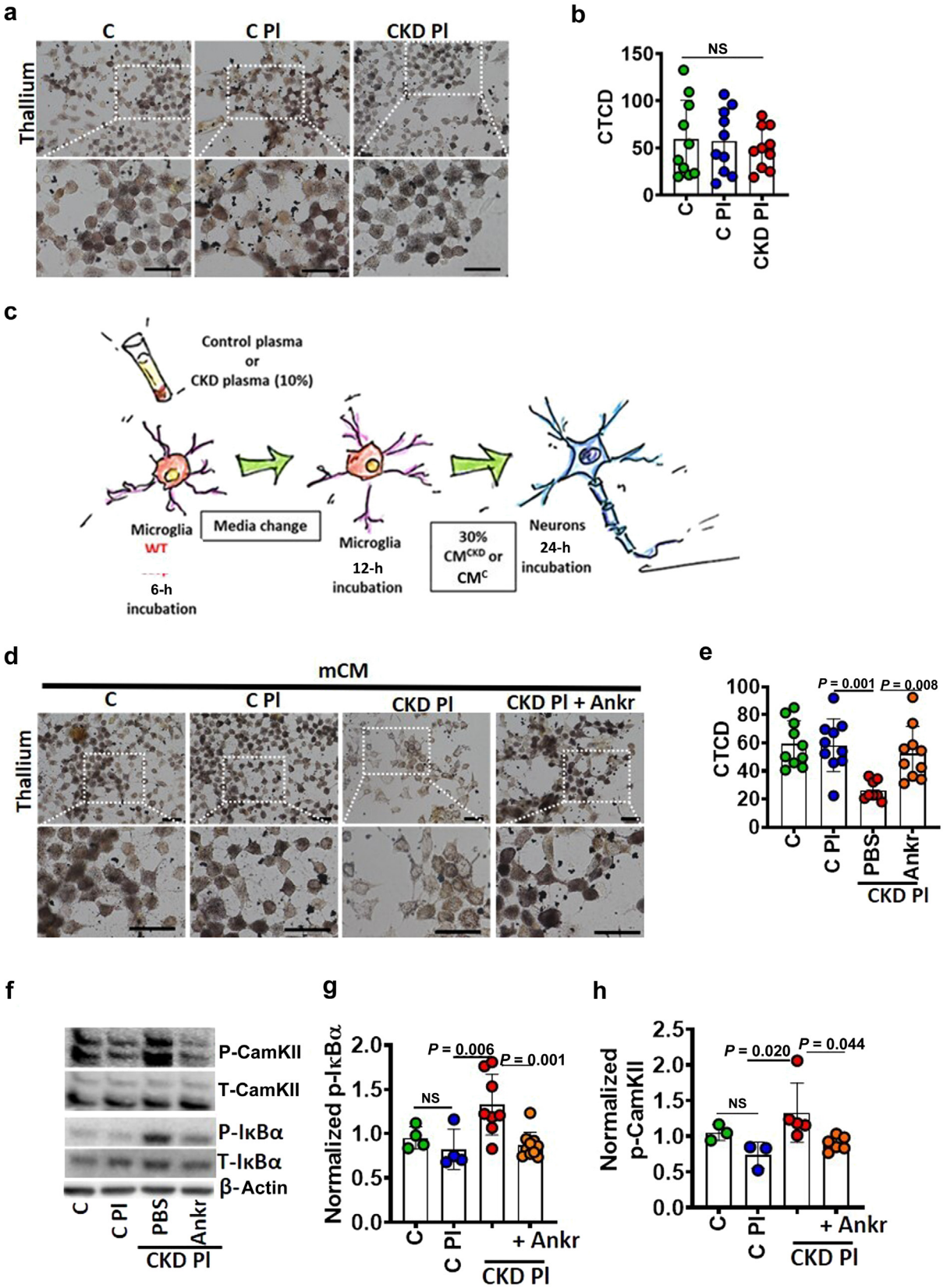

Figure 7 | Uremia-induced reduced neuronal potassium turnover depends on microglia-neuron crosstalk via interleukin-1β receptor 1. (**a,b**) Representative images (**a**) and bar graph with dot plot (each dot presents the corrected total cell density [CTCD] of stained cells in 1 field of view) (**b**) summarizing the results of thallium autometallography in neuronal cells. Cells were exposed to control plasma (C PI) or chronic kidney disease plasma (CKD PI). Bars = 50 μm. *P* values were determined using 1-way analysis of variance (ANOVA) (continued)

uptake in neurons (Figure 7a and b), suggesting that neuronal cells are not directly activated by uremia-dependent mediators.

Next, to determine whether altered Tl^+ uptake in neurons depends on a microglia-released mediator, we stimulated microglia with plasma from healthy controls or patients with CKD for 6 hours and replaced patients' plasma by fresh medium to obtain microglia-conditioned medium (mCM; Figure 7c). Exposing neuronal cells to mCM obtained from microglia pre-exposed to plasma of patients with CKD (mCM^{CKD}) reduced neuronal Tl^+ uptake, reflecting reduced potassium uptake, while CM from microglia pre-exposed to plasma from healthy controls (mCM^{C}) had no effect (Figure 7c–e). These observations suggest that in uremic conditions neuronal dysfunction depends on a factor released from activated microglia.

Considering the increased IL-1β generation in microglia exposed to CKD plasma, we hypothesized that IL-1β causes neuronal dysfunction. To this end, we stimulated neurons (Neuro-2a) with mCM^{C} or mCM^{CKD} without or with pre-exposure to the IL-1R antagonist anakinra (Ankr; mCM^{CKD}+Ankr). In the presence of Ankr (mCM^{CKD}+Ankr), mCM^{CKD} failed to reduce neuronal Tl^+ uptake. Additionally, while mCM^{CKD} induced phosphorylation of Ca2+/calmodulin-dependent protein kinase II (reflecting disturbed synaptic plasticity) and nuclear factor of κ light polypeptide gene enhancer in B-cell inhibitor-α (reflecting nuclear factor-κB activation; Figure 7d–h), these effects were not observed in the presence of Ankr, suggesting that IL-1β released from microglia induces neuronal dysfunction via IL-1R signaling.

To scrutinize the role of IL-1R1 signaling in neuronal dysfunction *in vivo*, we generated mice lacking IL-1R1 expression specifically in neurons ($Emx^{Cre} \times IL1R1^{LoxP/LoxP}$ mice, referred to as $IL1R^{\Delta N}$ mice; Figure 8a and b; Supplementary Figure S8A–D; Supplementary Table S4). On induction of CKD, neuronal thallium uptake was normalized in $IL1R^{\Delta N}$ mice, while thallium uptake in microglia of $IL1R^{\Delta N}$ CKD mice remained elevated (Figure 8c–e). This suggests that despite persistent microglia cell activation neurons lacking IL-1R1 remain unaffected, corroborating that IL-1β released from microglia acts on neurons via IL-1R1. Concurrently, despite persistently activated microglia, cognition was markedly improved in $IL1R^{\Delta N}$ CKD mice (Figure 8f and g). These data support a model in which IL-1β release from microglia drives IL-1R1–induced neuronal dysfunction and impaired cognition in CKD conditions.

To scrutinize whether the therapeutical application of the IL-1R inhibitor Ankr can rescue the impaired cognition observed in CKD mice, we treated sham or CKD mice with Ankr post induction of CKD (Supplementary Figure S8E). On induction of CKD, cognition was markedly improved in Ankr-treated mice (Figure 8h and i).

DISCUSSION

The mechanisms impairing cognition in patients with CKD remain largely elusive. Using a combination of mouse models, single-cell analyses, human samples, and *in vitro* experiments, we demonstrate impairment of the BBB, increased potassium efflux from microglia, and reduced neuronal potassium turnover, reflecting pathological activation of these brain cells in CKD. Our data suggest that potassium efflux from microglia triggers their activation, which results in release of IL-1β and IL-1R1–mediated neuronal dysfunction (as reflected by reduced neuronal potassium turnover). Importantly, inhibiting IL-1R signaling using Ankr prevented impairment of cognition in mice, suggesting that the pathway identified within this study can be pharmaceutically targeted. Thus, this study provides new mechanistic insight into cognitive impairment in association with CKD and identifies possible new therapeutic approaches.

The observed protection from impaired cognition in CKD mice lacking neuronal IL-1R1 is in agreement with previous reports showing a function of IL-1R1 in neuronal cells *in vitro*[15] or impaired cognition in association with an exaggerated inflammatory response of microglia with increased IL-1β secretion.[16] The protection from cognitive impairment in mice lacking neuronal IL-1R1 demonstrates that—at least in the model tested—neuronal dysfunction depends on neuronal IL-1R1 expression and paracrine (microglial) IL-1β secretion. Hence, blocking IL-1R1 may be a new therapeutic approach to mitigate CKD-induced cognitive impairment. However, long-term IL-1R1 inhibition may be detrimental, as full-body IL-1R1–deficient mice have cognitive deficits.[55] The latter illustrates that IL-1R1 has physiological effects in the brain, which may include functions of IL-1R1 for

Figure 7 | (continued) with Dunnett *post hoc* comparison. (**c**) Scheme summarizing the *in vitro* experimental approach: conditioned medium (CM) is generated by culture of microglia with C PI or CKD PI followed by washing the cells with phosphate-buffered saline (PBS) and adding standard medium. This medium is obtained after 12 hours and used as CM from controls (CM^{C}) or patients with CKD (CM^{CKD}) for further experiments with neuronal cells. (**d,e**) Representative images (**d**) and bar graph with dot plot (each dot presents the CTCD of stained cells in 1 field of view) (**e**) summarizing the results of thallium autometallography in neuronal cells. Cells were exposed to CM from microglial (mCM) pretreated with C PI or CKD PI with or without anakinra ([Ankr]; control: PBS solvent). Bar = 50 μm. *P* values were determined using 1-way ANOVA with Dunnett *post hoc* comparison. (**f**) Representative immunoblot images of neuronal cells incubated with CM from microglia treated with normal medium (C), C PI, or CKD PI without Ankr (CKD PI + PBS) or with Ankr (CKD PI + Ankr). Immunoblots for phospho-Ca^{2+}/calmodulin-dependent protein kinase II (P-CamKII) and phospho-nuclear factor of κ light polypeptide gene enhancer in B-cell inhibitor (P-IκBα) and respective total proteins are shown. (**g,h**) Quantification of immunoblots (bar graph, mean ± SEM; each dot represents 1 biological replicate) showing expression of P-CamKII (**g**) and P-IκBα (**h**) in neuronal cells. *P* values were determined using 1-way ANOVA with Dunnett *post hoc* comparison. NS, not significant; T-CamKII, total CamKII; T- IκBα, total IκBα; WT, wild type. To optimize viewing of this image, please see the online version of this article at www.kidney-international.org.

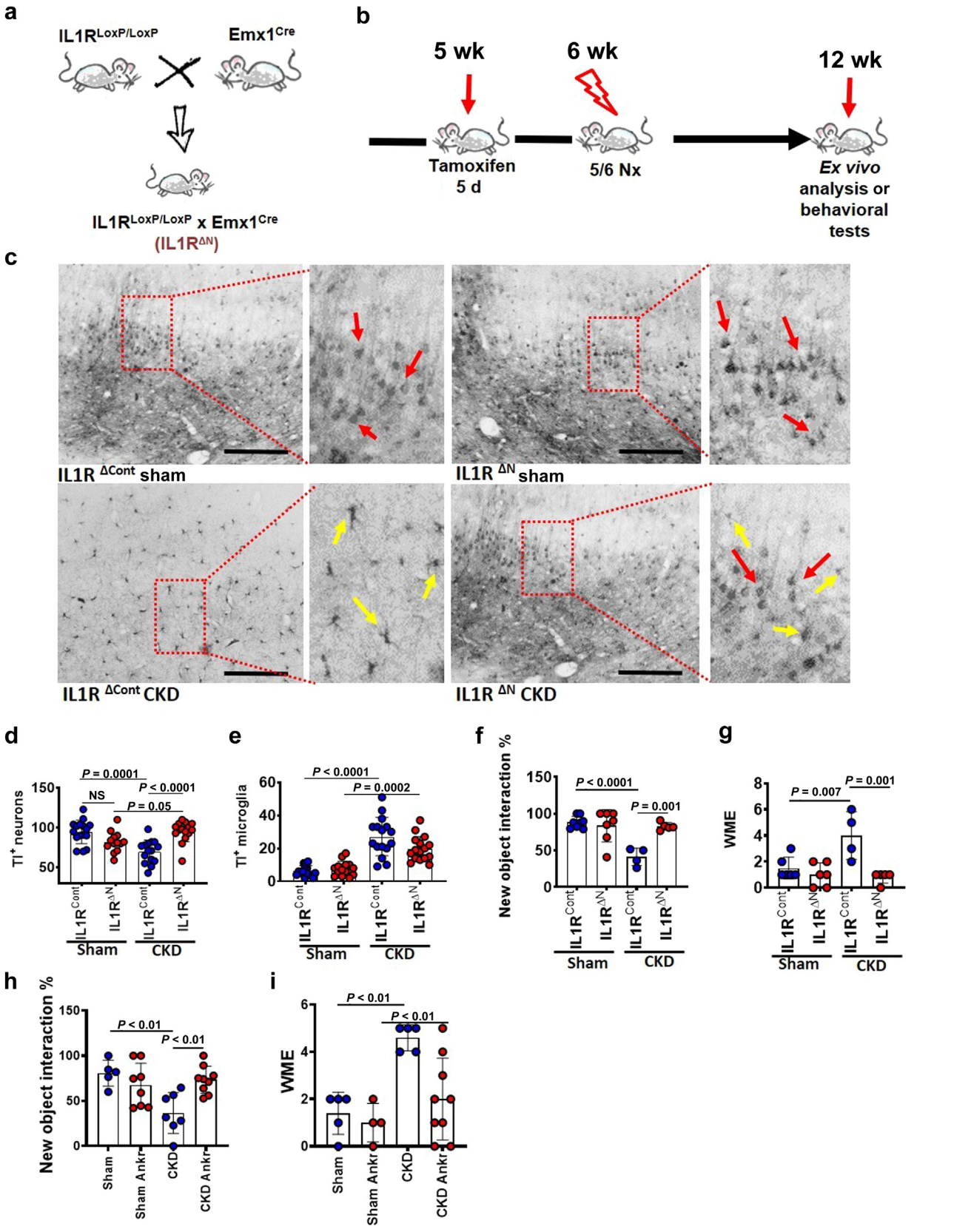

Figure 8 | Neuronal interleukin-1β receptor (IL-1R)–expression is required for uremia-induced cognitive impairment. (**a**) Scheme of conditional knock out of IL-1β receptor 1 (IL-1R1) in neuronal cells *in vivo* by crossing $Il1r1^{LoxP}$ mice to $Emx1^{Cre}$ mice, yielding $Il1R^{\Delta N}$ mice. (**b**) Experimental scheme showing 5-day injection period of tamoxifen, followed by 2-step 5/6 nephrectomy (5/6 Nx) surgery, (continued)

neurotransmission and synaptic plasticity.[56] Whether detrimental effects also occur if IL-1R1 is inhibited therapeutically in adulthood, possibly for a limited time or intermittently, remains to be shown. Yet, as systemic IL-1R1 inhibition may have unwanted side effects, caution is warranted and alternative therapeutic strategies may be needed.

Modulation of potassium efflux, a known inducer (primer) of inflammasome activation,[26] from microglia may constitute an alternative approach to restrict CKD-induced cognitive impairment, as suggested in the current study. The current data support a crucial role of the $K_{Ca}3.1$ channel for CKD-associated microglial potassium efflux and activation. Activation of the $K_{Ca}3.1$ channel induces microglial oxidative burst and nitric oxide production, reflecting microglia activation.[57] Thus, inhibition of $K_{Ca}3.1$, which is primarily expressed by microglia,[54,57] may constitute a possible new therapeutic approach to combat CKD-induced cognitive impairment. $K_{Ca}3.1$-knockout mice display mild volume dysregulation in erythrocytes, T cells, and mast cells but are healthy and have a normal life expectancy. $K_{Ca}3.1$ has been proposed as a drug target; its inhibition is safe in clinical studies,[54,57] and the $K_{Ca}3.1$ inhibitor senicapoc is currently evaluated in patients with Alzheimer's disease.[53] Inhibition of $K_{Ca}3.1$ reduces neuroinflammation in animal models of ischemic stroke, experimental autoimmune encephalomyelitis, and Alzheimer's disease,[53,58] but the underlying mechanisms remained unknown. The current study identifies a mechanism—inhibition of microglial IL-1β release and ensuing IL-1β–IL-1R1–triggered neuronal dysfunction—by which $K_{Ca}3.1$ inhibitors may maintain cognitive function. Providing that the use of senicapoc is safe in patients with CKD, further studies evaluating this new approach are warranted.

In the current study we demonstrate that the BBB is impaired in CKD mice, which may be an important pathogenetic step for CKD-induced impaired cognition. Increased vascular permeability in the brain, suggesting disruption of BBB, has been demonstrated after acute kidney injury, which was likewise associated with inflammation in the brain.[17,18] Breakdown of the BBB may be required for CKD-associated mediators to reach and activate microglia. Therefore, approaches to stabilize the BBB may constitute an additional therapeutic approach to combat cognitive impairment in CKD.

Like any study, the current study has limitations. We focused on microglia and neurons, because these cells depicted *in situ* potassium dyshomeostasis as detected by TlAMG. The release of IL-1β from microglia and the protection of neurons lacking IL-1R1 indicates a direct interaction of microglia and neurons via microglia IL-1β and neuronal IL-1R1. However, the snRNA-seq analyses suggest an increase of astrocytes, and hence we cannot exclude that other cell types, such as glia cells or astrocytes, contribute to IL-1R1–dependent signaling in neurons. Additionally, not only microglia but also oligodendrocytes and neurons express the hemoglobin scavenger CD163 following BBB disruption associated with intracranial hemorrhage.[39] Whether CD163 can be detected intracranially in chronic diseases associated with microvascular damage but without intracranial hemorrhage, such as in CKD, is not known so far. We did not detect the typical expression pattern of CD163 in the brain. Because CKD as a chronic disease is not—to the best of our knowledge—associated with bleeding into the brain parenchyma, we conclude that CD163 is not a suitable marker to detect impaired BBB function in CKD.

While we demonstrate that potassium efflux is required and may induce priming of inflammasome activation, which is congruent with the current paradigm of a 2-step inflammasome activation in immune cells,[59] we did not fully characterize the mechanism of IL-1β maturation in microglia. As others demonstrated that mice lacking inflammasome regulators such as NLRP3 are protected from neurodegenerative diseases,[60,61] it is tempting to speculate that the NLRP3 inflammasome is required for the second step of IL-1β maturation via caspase-1 cleavage. Yet, this needs to be formally tested in future studies.

In the current study we focused on CKD-induced impaired cognition by considering its clinical relevance. Additionally, we chose this model, because the cognitive impairment is independent of a primary defect in the central nervous system, such as in Alzheimer's disease, aiming to identify mechanisms in the absence of disease driving primary alterations within the brain itself. Yet, we acknowledge that the current results cannot be generalized to other peripheral diseases associated with cognitive impairment.

Additionally, while we show a pivotal role of the $K_{Ca}3.1$ channel for CKD-induced microglia activation and impaired cognition, other potassium channels may contribute to the potassium dyshomeostasis.[62,63] Yet, the current data demonstrate that—at least in mice—inhibiting the $K_{Ca}3.1$ channel is sufficient to protect from cognitive decline. Hence, in addition to targeting IL-1R signaling, it may be feasible to prevent

Figure 8 | (continued) followed by *ex vivo* analysis or behavioral tests. (**c–e**) Example images (**c**) and bar graph (mean ± SEM, each dot represents number of positive cells in 1 field of view; data from 4 different mice per group) with dot plot (**d,e**) summarizing thallium-positive (Tl+) cells in *ex vivo* thallium autometallography in the brains of IL-1R1 control ($IL1R^{Cont}$) and $IL1R^{\Delta N}$ CKD sham-operated control (sham) and CKD mice. Each dot represents the count of the respective cell type in 1 field of view. *P* values were determined using 1-way analysis of variance with Dunnett *post hoc* comparison; bar = 500 μm (**c**). Arrows depict microglia (yellow) or neurons (red). (**f,g**) Cognition, as determined by nonspatial object recognition ([NSOR]; the results are reported as the percentage of time spent with the new unknown object) (**f**) and radial arm maze ([RAM]; the results are reported as working memory errors [WMEs]) (**g**) tests summarized as bar graphs with dot plot (each dot representing 1 mouse) in $IL1R^{Cont}$ and $IL1R^{\Delta N}$ CKD sham-operated control and CKD mice. The data shown represent the mean ± SEM. (**h,i**) Cognition, as determined by NSOR (left; the results are reported as the percentage of time spent with the new unknown object) and RAM (right; the results are reported as WMEs) tests, in wild-type sham-operated control and CKD mice with or without treatment with anakinra (Ankr). NS, not significant. To optimize viewing of this image, please see the online version of this article at www.kidney-international.org.

CKD-associated impaired cognition by inhibiting the $K_{Ca}3.1$ channel and thus preventing microglia activation.

Lastly, in the current study we did not aim to identify a single uremic toxin impairing cognition in CKD. Considering the abundance of uremic toxins, we hypothesized that a rather larger number of uremic toxins impairs cognition. Hence, targeting a single uremic toxin is unlikely to solve the problem. Rather, we aimed to identify a "unifying" mechanism in the brain impairing cognition. We assumed that targeting such mechanism would be sufficient to ameliorate CKD-induced impaired cognition irrespective of the number of uremic toxins involved. This aim was achieved at least in the mouse model used.

In the current study we propose that a potassium efflux from microglia triggers IL-1 β release from microglia. We cannot exclude that the release of potassium from microglia modulates neuronal function.[64,65] Other cells, such as astrocytes, may buffer electrolytes, rendering the analyses of dynamically altered electrolytes in the brain in the presence of CKD more complex. Importantly, we demonstrate that neuronal IL-1R1 deficiency is sufficient to ameliorate CKD-induced impaired cognition. The improvement of cognition in neuronal IL-1R1–deficient mice despite CKD provides strong evidence for a pivotal role neuronal IL-1β–IL-1R1 signaling irrespective of possible concomitant alterations in intercellular electrolytes in CKD-induced cognitive impairment.

In summary, the current study unravels a role of potassium dyshomeostasis in IL-1β release from microglia and identifies a crucial function of neuronal IL-1R1 for impairing cognition in CKD. These data provide new insights into CKD-associated impaired cognition and are expected to spur studies (i) addressing the relevance of this mechanism in other neurodegenerative diseases, (ii) identifying further mechanistic details, and (iii) evaluating therapeutic approaches combating CKD-associated impaired cognition.

DISCLOSURE

All the authors declared no competing interests.

DATA STATEMENT

Patient data, statistics, and methods are publicly available in the Methods section or the Supplementary Materials. The data that support the findings of this study are available on reasonable request. Raw data from the snRNA-seq analyses have been uploaded to the GEO under the accession number GSE218613. The code used in the analyses (RNA-seq data) is available in the github repository: https://github.com/silkezimm/seurat_code. For general comments or material requests please contact SZ (silke.zimmermann@medizin.uni-leipzig.de) or BI (berend.isermann@medizin.uni-leipzig.de).

ACKNOWLEDGMENTS

We thank Kathrin Deneser, Rumiya Makarova, Raik Rönicke, Susanne von Kenne, and Monika Riek-Burchardt for excellent technical support and Prof. Dr. Marc Schönwiesner and Dr. med. Martin Krüger for their support.

FUNDING

This work was funded by Deutsche Forschungsgemeinschaft (DFG, German Research Foundation) grants IS-67/16-1, IS-67/22-1, IS-67/25-1, IS-67/26-1, SFB854/B26, 361210922/GRK2408/P7&P9 (to BI), 361210922/GRK2408/P5 and SH 849/1-2 (to KS), KO 5736/1-1 (to SK), and 457240345 (to BS); Deutscher Akademischer Austauschdienst (DAAD, German Academic Exchange Service) scholarships (to AE); and the Medical Faculty of the University of Leipzig (to SZ).

AUTHOR CONTRIBUTIONS

SZ performed *in vivo, in vitro*, and *ex vivo* experiments. AM and AE assisted in performing *in vivo* studies and *ex vivo* analyses. KhS, SDS, and TR assisted in animal work and documentation. SZ, OB, and BNS conducted expression analyses and data interpretation. SZ and OB conducted functional annotation, data analyses, and *in silico* studies. CM provided human brain sections and interpreted data. JG provided reagents, expertise, and interpreted data (TIAMG). SJ, KW, RR, and KuS assisted in *ex vivo* and *in vitro* analyses. AM, SK, RB, UK, and I.B assisted in review and editing of the manuscript and interpretation. SZ and BI conceptually designed and interpreted the experimental work and prepared the manuscript.

Supplementary material is available online at www.kidney-international.org.

REFERENCES

1. Drew DA, Weiner DE, Sarnak MJ. Cognitive impairment in CKD: pathophysiology, management, and prevention. *Am J Kidney Dis*. 2019;74:782–790.
2. Kachaamy T, Bajaj JS. Diet and cognition in chronic liver disease. *Curr Opin Gastroenterol*. 2011;27:174–179.
3. Kurella M, Chertow GM, Luan J, Yaffe K. Cognitive impairment in chronic kidney disease. *J Am Geriatr Soc*. 2004;52:1863–1869.
4. Radić J, Ljutić D, Radić M, et al. Kidney transplantation improves cognitive and psychomotor functions in adult hemodialysis patients. *Am J Nephrol*. 2011;34:399–406.
5. van Sandwijk MS, Berge IJM ten, Caan MWA, et al. Cognitive improvement after kidney transplantation is associated with structural and functional changes on MRI. *Transplant Direct*. 2020;6:e531.
6. Pantiga C, Rodrigo LR, Cuesta M, et al. Cognitive deficits in patients with hepatic cirrhosis and in liver transplant recipients. *J Neuropsychiatry Clin Neurosci*. 2003;15:84–89.
7. Cserép C, Pósfai B, Lénárt N, et al. Microglia monitor and protect neuronal function through specialized somatic purinergic junctions. *Science*. 2020;367:528–537.
8. Parkhurst CN, Yang G, Ninan I, et al. Microglia promote learning-dependent synapse formation through brain-derived neurotrophic factor. *Cell*. 2013;155:1596–1609.
9. Shein NA, Grigoriadis N, Horowitz M, et al. Microglial involvement in neuroprotection following experimental traumatic brain injury in heat-acclimated mice. *Brain Res*. 2008;1244:132–141.
10. Niu L, Luo SS, Xu Y, et al. The critical role of the hippocampal NLRP3 inflammasome in social isolation-induced cognitive impairment in male mice. *Neurobiol Learn Mem*. 2020;175:107301.
11. Stoll G, Jander S, Schroeter M. Detrimental and beneficial effects of injury-induced inflammation and cytokine expression in the nervous system. *Adv Exp Med Biol*. 2002;513:87–113.
12. Hauptmann J, Johann L, Marini F, et al. Interleukin-1 promotes autoimmune neuroinflammation by suppressing endothelial heme oxygenase-1 at the blood-brain barrier. *Acta Neuropathol*. 2020;140:549–567.
13. Viviani B, Boraso M, Marchetti N, Marinovich M. Perspectives on neuroinflammation and excitotoxicity: a neurotoxic conspiracy? *Neurotoxicology*. 2014;43:10–20.
14. Vezzani A, Viviani B. Neuromodulatory properties of inflammatory cytokines and their impact on neuronal excitability. *Neuropharmacology*. 2015;96:70–82.

15. Skelly DT, Griffin ÉW, Murray CL, et al. Acute transient cognitive dysfunction and acute brain injury induced by systemic inflammation occur by dissociable IL-1-dependent mechanisms. *Mol Psychiatry*. 2019;24:1533–1548.
16. Daniels MJD, Rivers-Auty J, Schilling T, et al. Fenamate NSAIDs inhibit the NLRP3 inflammasome and protect against Alzheimer's disease in rodent models. *Nat Commun*. 2016;7:12504.
17. Liu M, Liang Y, Chigurupati S, et al. Acute kidney injury leads to inflammation and functional changes in the brain. *J Am Soc Nephrol*. 2008;19:1360–1370.
18. Salama M, Farrag SM, Abulasrar SA, et al. Up-regulation of TLR-4 in the brain after ischemic kidney-induced encephalopathy in the rat. *CNS Neurol Disord Drug Targets*. 2013;12:583–586.
19. Hernandez L, Ward LJ, Arefin S, et al. Blood-brain barrier and gut barrier dysfunction in chronic kidney disease with a focus on circulating biomarkers and tight junction proteins. *Sci Rep*. 2022;12:4414.
20. Yang Y, Rosenberg GA. Blood-brain barrier breakdown in acute and chronic cerebrovascular disease. *Stroke*. 2011;42:3323–3328.
21. Sweeney MD, Sagare AP, Zlokovic BV. Blood-brain barrier breakdown in Alzheimer disease and other neurodegenerative disorders. *Nat Rev Neurol*. 2018;14:133–150.
22. Lim YJ, Sidor NA, Tonial NC, Che A, Urquhart BL. Uremic toxins in the progression of chronic kidney disease and cardiovascular disease: mechanisms and therapeutic targets. *Toxins (Basel)*. 2021;13:142.
23. Heneka MT, Kummer MP, Stutz A, et al. NLRP3 is activated in Alzheimer's disease and contributes to pathology in APP/PS1 mice. *Nature*. 2013;493:674–678.
24. Heneka MT, McManus RM, Latz E. Inflammasome signalling in brain function and neurodegenerative disease. *Nat Rev Neurosci*. 2018;19:610–621.
25. Butterworth RF. Hepatic encephalopathy in cirrhosis: pathology and pathophysiology. *Drugs*. 2019;79(suppl 1):17–21.
26. Gaidt MM, Hornung V. Alternative inflammasome activation enables IL-1β release from living cells. *Curr Opin Immunol*. 2017;44:7–13.
27. Bock F, Shahzad K, Wang H, et al. Activated protein C ameliorates diabetic nephropathy by epigenetically inhibiting the redox enzyme p66Shc. *Proc Natl Acad Sci U S A*. 2013;110:648–653.
28. Gross O, Poeck H, Bscheider M, et al. Syk kinase signalling couples to the Nlrp3 inflammasome for anti-fungal host defence. *Nature*. 2009;459:433–436.
29. Radloff J, Latic N, Pfeiffenberger U, et al. A phosphate and calcium-enriched diet promotes progression of 5/6-nephrectomy-induced chronic kidney disease in C57BL/6 mice. *Sci Rep*. 2021;11:14868.
30. Schubert D, Humphreys S, Vitry F de, Jacob F. Induced differentiation of a neuroblastoma. *Dev Biol*. 1971;25:514–546.
31. Deng A, Arndt MAK, Satriano J, et al. Renal protection in chronic kidney disease: hypoxia-inducible factor activation vs. angiotensin II blockade. *Am J Physiol Renal Physiol*. 2010;299:F1365–F1373.
32. Kujal P, Vernerová Z. Model 5/6 nefrektomie, jako experimentální model chronické renální insuficience a adaptace ledvin na redukci poctu nefronů. *Cesk Fysiol*. 2008;57:104–109.
33. Villeda SA, Plambeck KE, Middeldorp J, et al. Young blood reverses age-related impairments in cognitive function and synaptic plasticity in mice. *Nat Med*. 2014;20:659–663.
34. Castellano JM, Mosher KI, Abbey RJ, et al. Human umbilical cord plasma proteins revitalize hippocampal function in aged mice. *Nature*. 2017;544:488–492.
35. Goldschmidt J, Wanger T, Engelhorn A, et al. High-resolution mapping of neuronal activity using the lipophilic thallium chelate complex TlDDC: protocol and validation of the method. *Neuroimage*. 2010;49:303–315.
36. Mazumder MK, Giri A, Kumar S, Borah A. A highly reproducible mice model of chronic kidney disease: evidences of behavioural abnormalities and blood-brain barrier disruption. *Life Sci*. 2016;161:27–36.
37. Karperien A, Ahammer H, Jelinek HF. Quantitating the subtleties of microglial morphology with fractal analysis. *Front Cell Neurosci*. 2013;7:3.
38. Crews FT, Sarkar DK, Qin L, et al. Neuroimmune function and the consequences of alcohol exposure. *Alcohol Res*. 2015;37:331–341, 344–351.
39. Jing C, Zhang H, Shishido H, et al. Association of brain CD163 expression and brain injury/hydrocephalus development in a rat model of subarachnoid hemorrhage. *Front Neurosci*. 2018;12:313.
40. Pey P, Pearce RKB, Kalaitzakis ME, et al. Phenotypic profile of alternative activation marker CD163 is different in Alzheimer's and Parkinson's disease. *Acta Neuropathol Commun*. 2014;2:21.
41. Ma J, Wang B, Wei X, et al. Accumulation of extracellular elastin-derived peptides disturbed neuronal morphology and neuron-microglia crosstalk in aged brain. *J Neurochem*. 2024;168:1460–1474.
42. Ronzano R, Roux T, Thetiot M, et al. Microglia-neuron interaction at nodes of Ranvier depends on neuronal activity through potassium release and contributes to remyelination. *Nat Commun*. 2021;12:5219.
43. Lee H-M, Kang J, Lee SJ, Jo E-K. Microglial activation of the NLRP3 inflammasome by the priming signals derived from macrophages infected with mycobacteria. *Glia*. 2013;61:441–452.
44. Duan Y, Kelley N, He Y. Role of the NLRP3 inflammasome in neurodegenerative diseases and therapeutic implications. *Neural Regen Res*. 2020;15:1249–1250.
45. Venegas C, Heneka MT. Inflammasome-mediated innate immunity in Alzheimer's disease. *FASEB J*. 2019;33:13075–13084.
46. Qu J, Tao X-Y, Teng P, et al. Blocking ATP-sensitive potassium channel alleviates morphine tolerance by inhibiting HSP70-TLR4-NLRP3-mediated neuroinflammation. *J Neuroinflammation*. 2017;14:228.
47. Chung Y-H, Kim D-H, Lee W-W. Monosodium urate crystal-induced pro-interleukin-1β production is post-transcriptionally regulated via the p38 signaling pathway in human monocytes. *Sci Rep*. 2016;6:34533.
48. Schilling T, Lehmann F, Rückert B, Eder C. Physiological mechanisms of lysophosphatidylcholine-induced de-ramification of murine microglia. *J Physiol*. 2004;557:105–120.
49. Khanna R, Roy L, Zhu X, Schlichter LC. K+ channels and the microglial respiratory burst. *Am J Physiol Cell Physiol*. 2001;280:C796–C806.
50. Kaushal V, Koeberle PD, Wang Y, Schlichter LC. The Ca2+-activated K+ channel KCNN4/KCa3.1 contributes to microglia activation and nitric oxide-dependent neurodegeneration. *J Neurosci*. 2007;27:234–244.
51. Chen Y-J, Raman G, Bodendiek S, et al. The KCa3.1 blocker TRAM-34 reduces infarction and neurological deficit in a rat model of ischemia/reperfusion stroke. *J Cereb Blood Flow Metab*. 2011;31:2363–2374.
52. Maezawa I, Zimin PI, Wulff H, Jin L-W. Amyloid-beta protein oligomer at low nanomolar concentrations activates microglia and induces microglial neurotoxicity. *J Biol Chem*. 2011;286:3693–3706.
53. Jin L-W, Di Lucente J, Nguyen HM, et al. Repurposing the KCa3.1 inhibitor senicapoc for Alzheimer's disease. *Ann Clin Transl Neurol*. 2019;6:723–738.
54. Brown BM, Pressley B, Wulff H. KCa3.1 channel modulators as potential therapeutic compounds for glioblastoma. *Curr Neuropharmacol*. 2018;16:618–626.
55. Avital A, Goshen I, Kamsler A, et al. Impaired interleukin-1 signaling is associated with deficits in hippocampal memory processes and neural plasticity. *Hippocampus*. 2003;13:826–834.
56. White CS, Lawrence CB, Brough D, Rivers-Auty J. Inflammasomes as therapeutic targets for Alzheimer's disease. *Brain Pathol*. 2017;27:223–234.
57. Wulff H, Castle NA. Therapeutic potential of KCa3.1 blockers: recent advances and promising trends. *Expert Rev Clin Pharmacol*. 2010;3:385–396.
58. Maezawa I, Jenkins DP, Jin BE, Wulff H. Microglial KCa3.1 channels as a potential therapeutic target for Alzheimer's disease. *Int J Alzheimers Dis*. 2012;2012:868972.
59. van Hout GPJ, Bosch L. The inflammasomes in cardiovascular disease. *Exp Suppl*. 2018;108:9–40.
60. Li J-M, Hu T, Zhou X-N, et al. The involvement of NLRP3 inflammasome in CUMS-induced AD-like pathological changes and related cognitive decline in mice. *J Neuroinflammation*. 2023;20:112.
61. Jha S, Srivastava SY, Brickey WJ, et al. The inflammasome sensor, NLRP3, regulates CNS inflammation and demyelination via caspase-1 and interleukin-18. *J Neurosci*. 2010;30:15811–15820.
62. Di Lucente J, Nguyen HM, Wulff H, et al. The voltage-gated potassium channel Kv1.3 is required for microglial pro-inflammatory activation in vivo. *Glia*. 2018;66:1881–1895.
63. Vay SU, Flitsch LJ, Rabenstein M, et al. The impact of hyperpolarization-activated cyclic nucleotide-gated (HCN) and voltage-gated potassium KCNQ/Kv7 channels on primary microglia function. *J Neuroinflammation*. 2020;17:100.
64. Arbabi K, Jiang Y, Howard D, et al. Investigating microglia-neuron crosstalk by characterizing microglial contamination in human and mouse patch-seq datasets. *iScience*. 2023;26:107329.
65. Chang RC, Hudson PM, Wilson BC, et al. High concentrations of extracellular potassium enhance bacterial endotoxin lipopolysaccharide-induced neurotoxicity in glia-neuron mixed cultures. *Neuroscience*. 2000;97:757–764.